

CONSTRAINTS ON LONG-BASELINE NEUTRINO  
OSCILLATION PROBABILITIES AND CP ASYMMETRIES  
FROM NEUTRINO OSCILLATION DATA

S.M. Bilenky

Joint Institute for Nuclear Research, Dubna, Russia, and  
Technion, Physics Department, 32000 Haifa, Israel.

C. Giunti

INFN, Sezione di Torino, and Dipartimento di Fisica Teorica, Università di Torino,  
Via P. Giuria 1, I-10125 Torino, Italy.

W. Grimus

Institute for Theoretical Physics, University of Vienna,  
Boltzmanngasse 5, A-1090 Vienna, Austria.

Abstract

We consider long-baseline neutrino oscillations in the framework of two schemes with mixing of four massive neutrinos which can accommodate all the existing indications in favour of neutrino mixing. Within these schemes, we derive bounds on the oscillation probabilities and the CP-odd neutrino-antineutrino asymmetries in long-baseline experiments. Using the results of short-baseline neutrino oscillation experiments, we obtain rather strong upper bounds on the long-baseline probabilities  $1 - P_{e!e}^{(LBL)}$  and  $P_{(\nu)!(\nu)}^{(LBL)}$ . Nevertheless, the projected sensitivities of the MINOS and ICARUS experiments are better than our bounds. We also show that there are no corresponding constraints for  $(\nu)!(\nu)$  and  $(\nu)!(\nu)$  long-baseline oscillations and that the CP-odd asymmetry in the latter channel can reach the maximal value  $2/3 - 1/3$  allowed by the unitarity of the mixing matrix. Some schemes with mixing of three neutrinos are also considered.

14.60Pq, 14.60St

## I. INTRODUCTION

The search for neutrino oscillations remains a central issue of neutrino experiments. In several short-baseline (SBL) experiments, which are sensitive to relatively large values of the neutrino mass-squared difference  $m^2$  ( $m^2 \sim 0.1 \text{ eV}^2$ ), different oscillation channels are investigated at present:  $\nu_e \rightarrow \nu_e$  (LSND [1], KARMEN [2], CCFR [3], NOMAD [4]);  $\nu_e \rightarrow \nu_\mu$  (CHORUS [5], NOMAD [6] and CCFR [7]). The long-baseline (LBL) neutrino oscillation experiments which will operate in the near future will be sensitive to much smaller values of  $m^2$  ( $m^2 \sim 10^{-3} \text{ eV}^2$ ). Long-baseline experiments with reactor antineutrinos are starting to take data (CHOOZ [8]) or are under preparation (Pal Verde [9]). Long-baseline experiments with accelerator neutrinos (KEK {Super-Kamiokande [10], Fermilab {Soudan [11], CERN {Gran Sasso [12]) are under preparation.

No indications in favour of neutrino oscillations have been found in many experiments with terrestrial neutrinos which have been done in the past (see the reviews in Ref. [13]). On the other hand, such indications have been found in all solar neutrino experiments (Homestake, Kamiokande, GALLEX and SAGE [14]). The suppression of the detected event rates with respect to those predicted by the Standard Solar Model (SSM) [15] can be explained with neutrino mixing. In the case of resonant MSW transitions [16], it was found [17] that the oscillation parameters  $m^2$  and  $\sin^2 2\theta$  ( $\theta$  is the mixing angle) have the following values:

$$3 \cdot 10^6 \cdot m^2 \cdot 1.2 \cdot 10^5 \text{ eV}^2; \quad 4 \cdot 10^3 \cdot \sin^2 2\theta \cdot 1.2 \cdot 10^2 : \quad (1.1)$$

The solar neutrino puzzle can also be solved by invoking vacuum neutrino oscillations [18], in which case  $m^2 \sim 10^{10} \text{ eV}^2$ .

Indications in favour of  $\nu_e \rightarrow \nu_x$  oscillations ( $x \neq e$ ) have been found also in the Kamiokande [19], IMB [20] and Soudan [21] atmospheric neutrino experiments. From the analysis of the Kamiokande data the following allowed ranges for the oscillation parameters were obtained [19]:

$$5 \cdot 10^3 \cdot m^2 \cdot 3 \cdot 10^2 \text{ eV}^2; \quad 0.7 \cdot \sin^2 2\theta \cdot 1 \quad ( \quad ); \quad (1.2)$$

$$7 \cdot 10^3 \cdot m^2 \cdot 8 \cdot 10^2 \text{ eV}^2; \quad 0.6 \cdot \sin^2 2\theta \cdot 1 \quad ( \quad e ); \quad (1.3)$$

Finally, indications in favour of  $\nu_e \rightarrow \nu_\tau$  oscillations have been found recently in the LSND experiment [1], in which antineutrinos originating from the decays of  $\mu^+$ 's at rest were detected. From the analysis of the data of this experiment and the negative results of other SBL experiments (in particular, the Bugey [22] and BNL E776 [23] experiments), it follows that

$$0.3 \cdot m^2 \cdot 2.2 \text{ eV}^2; \quad 10^3 \cdot \sin^2 2\theta \cdot 4 \cdot 10^2 : \quad (1.4)$$

All the above-mentioned hints for neutrino oscillations can be accommodated in schemes with four neutrinos. These schemes require a sterile neutrino field ( $\nu_s$ ) in addition to the usual flavour fields with flavours  $\nu = e, \mu, \tau$ . The specific nature of such 4-neutrino schemes has recently been derived from the data [24,25].



where  $m_{k1}^2 = m_k^2 - m_1^2$  (we take  $m_1 < m_2 < \dots$ ). From Eqs.(2.2) and (2.3) it follows that the transition probabilities of neutrinos and antineutrinos are connected by the relation

$$P_{\nu_i \nu_j} = P_{\bar{\nu}_i \bar{\nu}_j} \quad (2.4)$$

This relation reflects CPT invariance.

If CP invariance in the lepton sector holds, then there are phase conventions such that in the case of Dirac neutrinos we have

$$U_k = U_k^* \quad (2.5)$$

whereas in the case of Majorana neutrinos we have

$$U_k = \eta_k U_k^* \quad (2.6)$$

where  $\eta_k = \pm i$  is the CP parity<sup>1</sup> of the Majorana neutrino with mass  $m_k$  (see, for example, Ref. [30]). It is obvious that the CP parities  $\eta_k$  do not enter in the expressions for the transition amplitudes. Hence, in both the Dirac and Majorana cases, CP invariance implies that [33]

$$P_{\nu_i \nu_j} = P_{\bar{\nu}_i \bar{\nu}_j} \quad (2.7)$$

Let us introduce the CP-odd asymmetries

$$D_{ij} = P_{\nu_i \nu_j} - P_{\bar{\nu}_i \bar{\nu}_j} \quad (2.8)$$

From CPT invariance it follows that

$$D_{ij} = -D_{ji} \quad (2.9)$$

Furthermore, from the unitarity of the mixing matrix we have

$$\sum_k D_{ij} = 0 \quad (2.10)$$

We observe that in the case of transitions among three flavour states ( $\nu_e, \nu_\mu, \nu_\tau$ ) the CP asymmetries satisfy the relations [34]

$$D_{e\mu} = D_{\mu\tau} = D_{\tau e} \quad (2.11)$$

which follow from Eqs.(2.9) and (2.10).

In the general case of mixing of an arbitrary number of massive neutrinos, the asymmetries are given by

$$D_{ij} = 4 \sum_{k>j} \text{Im} U_{ij} U_{jk} U_{ki} \sin \frac{m_{kj}^2 L}{2p} \quad (2.12)$$

Therefore, CP violation in the lepton sector can be observed only if at least one of the oscillating terms in the transition probabilities does not vanish due to the averaging over the neutrino energy spectrum and the size of the neutrino source and detector.

---

<sup>1</sup> The CP parities of Majorana neutrinos could be important for neutrinoless double beta-decay; for example, if the  $\eta_k$ 's have different CP parities, their contributions to the amplitude of neutrinoless double-beta decay could cancel each other [32].

### III. FOUR MASSIVE NEUTRINOS

All existing indications in favour of neutrino oscillations can be accommodated by a scheme with mixing of four massive neutrinos [35,36,24,25]. In Ref. [24] we have shown that from the six possible spectral schemes of four massive neutrinos, which correspond to three different scales of mass-squared differences  $m_{kj}^2$ , only two schemes are compatible with the results of all experiments. In these two schemes the four neutrino masses are divided in two pairs of close masses separated by a gap of  $\sim 1$  eV :

$$(A) \quad \underbrace{\left. \begin{array}{l} \underbrace{m_1 < m_2}_{\text{LSND}} \\ \underbrace{m_3 < m_4}_{\text{LSND}} \end{array} \right\} \left. \begin{array}{l} \text{atm} \\ \text{solar} \end{array} \right\}}_{\text{LSND}} \quad \text{and} \quad (B) \quad \underbrace{\left. \begin{array}{l} \underbrace{m_1 < m_2}_{\text{LSND}} \\ \underbrace{m_3 < m_4}_{\text{LSND}} \end{array} \right\} \left. \begin{array}{l} \text{solar} \\ \text{atm} \end{array} \right\}}_{\text{LSND}} : \quad (3.1)$$

In scheme A,  $m_{21}^2$  is relevant for the explanation of the atmospheric neutrino anomaly and  $m_{43}^2$  is relevant for the suppression of solar  $\nu_e$ 's. In scheme B, the roles of  $m_{21}^2$  and  $m_{43}^2$  are reversed.

We will consider first SBL neutrino oscillations in the framework of these two schemes. Let us note above all that it is impossible to reveal the effects of CP violation in these experiments which are sensitive to  $m_{41}^2 \sim 0.1 \text{ eV}^2$ . Furthermore, both schemes A and B give the same oscillation probabilities. Therefore, it is impossible to distinguish A from B in SBL oscillation experiments either. In fact, since in these experiments

$$\frac{m_{21}^2 L}{2p} \ll 1 \quad \text{and} \quad \frac{m_{43}^2 L}{2p} \ll 1 ; \quad (3.2)$$

the probabilities of  $\nu \rightarrow \nu$  and  $\bar{\nu} \rightarrow \bar{\nu}$  transitions are equal and are given by [36]

$$P_{(\nu) \rightarrow (\nu)}^{(SBL)} = \frac{1}{2} A ; \quad 1 - \cos \frac{m^2 L}{2p} ; \quad (3.3)$$

with  $m^2 = m_{41}^2 = m_{42}^2 = m_{43}^2$  and the oscillation amplitude

$$A ; = 4 \sum_{k=1;2} U_{k1} U_{k1}^2 = 4 \sum_{k=3;4} U_{k1} U_{k1}^2 : \quad (3.4)$$

The survival probabilities of neutrinos and antineutrinos are given by

$$P_{(\nu) \rightarrow (\nu)}^{(SBL)} = 1 - \sum_{\mu} P_{(\nu) \rightarrow (\mu)}^{(SBL)} = 1 - \frac{1}{2} B ; \quad 1 - \cos \frac{m^2 L}{2p} ; \quad (3.5)$$

where

$$B ; = \sum_{\mu} A ; = 4 \sum_{k=1;2} |U_{k1}|^2 = 1 - 4 \sum_{k=1;2} |U_{k1}|^2 = 4 \sum_{k=3;4} |U_{k1}|^2 = 1 - 4 \sum_{k=3;4} |U_{k1}|^2 : \quad (3.6)$$

Long-baseline neutrino oscillation experiments are planned to be sensitive to the "atmospheric neutrino range"  $10^3 \text{ eV}^2 \lesssim m_{kj}^2 \lesssim 10^4 \text{ eV}^2$ . In scheme A, the probabilities of  $\nu_i \rightarrow \nu_j$  and  $\bar{\nu}_i \rightarrow \bar{\nu}_j$  transitions in LBL experiments are given by

$$P_{ij}^{(\text{LBL},\text{A})} = U_{1i} U_{1j} + U_{2i} U_{2j} \exp \left[ -i \frac{m_{21}^2 L}{2p} \right] + \sum_{k=3,4} U_{ki} U_{kj} \exp \left[ -i \frac{m_{kj}^2 L}{2p} \right]; \quad (3.7)$$

$$P_{ij}^{(\text{LBL},\text{B})} = U_{1i} U_{1j} + U_{2i} U_{2j} \exp \left[ -i \frac{m_{21}^2 L}{2p} \right] + \sum_{k=3,4} U_{ki} U_{kj} \exp \left[ -i \frac{m_{kj}^2 L}{2p} \right]; \quad (3.8)$$

These formulas have been obtained from Eqs.(2.2) and (2.3), respectively, taking into account the fact that in LBL experiments  $m_{43}^2 L = 2p \gg 1$  and dropping the terms proportional to the cosines of phases much larger than  $2\pi$  ( $m_{kj}^2 L = 2p \gg 2\pi$  for  $k = 3,4$  and  $j = 1,2$ ). Such terms do not contribute to the oscillation probabilities averaged over the neutrino energy spectrum. The transition probabilities in scheme B ensue from the expressions (3.7) and (3.8) with the change

$$1;2 \leftrightarrow 3;4; \quad (3.9)$$

From Eqs.(3.7), (3.8) and (3.9) it follows that the LBL CP-odd asymmetries  $D_{ij}^{(\text{LBL})}$  in the schemes A and B are given by

$$D_{ij}^{(\text{LBL},\text{A})} = I^{(\text{A})} \sin \frac{m_{21}^2 L}{2p}; \quad (3.10)$$

$$D_{ij}^{(\text{LBL},\text{B})} = I^{(\text{B})} \sin \frac{m_{43}^2 L}{2p}; \quad (3.11)$$

with the oscillation amplitudes

$$I^{(\text{A})} = 4 \text{Im} U_{11} U_{12} U_{21} U_{22}; \quad I^{(\text{B})} = 4 \text{Im} U_{33} U_{34} U_{43} U_{44}; \quad (3.12)$$

We will now discuss the constraints on the neutrino oscillation parameters which follow from the existing results of SBL experiments. In the disappearance SBL reactor and accelerator experiments no indication in favour of neutrino oscillations was found (see the reviews in Ref. [13]). At any fixed value of  $m^2$  in the range

$$0.1 \text{ eV}^2 \lesssim m^2 \lesssim 10^3 \text{ eV}^2; \quad (3.13)$$

from the exclusion plots of the Bugey [22]  $\bar{\nu}_e$  disappearance experiment and of the CDHS [37] and CCFR [38]  $\nu_\mu$  disappearance experiments we have

$$|B_{ij}| \leq B_{ij}^0, \quad (i, j = e; \mu); \quad (3.14)$$

Let us define the quantities  $c_{ij}$  (with  $i, j = e; \mu$ ) in the two schemes A and B as

$$(A) \quad c_{ij} = \sum_{k=1,2} U_{ki} U_{kj}^2; \quad (3.15)$$

$$(B) \quad c_{ij} = \sum_{k=3,4} U_{ki} U_{kj}^2; \quad (3.16)$$

Taking also into account the results of the solar neutrino experiments and the results of the atmospheric neutrino experiments, in both schemes A and B, the quantities  $c_e$  and  $c$  are constrained by [24]

$$c_e \leq a_e^0; \quad c \leq 1 - a^0; \quad (3.17)$$

where

$$a^0 = \frac{1}{2} \left( 1 + \sqrt{1 - 4B^0} \right); \quad (\nu = e; \mu); \quad (3.18)$$

The values of  $a_e^0$  and  $a^0$  which have obtained from the exclusion plots of the Bugey [22], CDHS [37] and CCFR [38] experiments are given in Fig.1 of Ref. [39]. For values of  $m^2$  in the range (3.13)  $a_e^0$  is small ( $a_e^0 \leq 4 \cdot 10^{-2}$ ), and  $a^0$  is small for  $m^2 \leq 0.3 \text{ eV}^2$  ( $a^0 \leq 10^{-1}$ ). In the following we will use also the limits on the amplitudes  $A_{\nu\mu}$ , which can be obtained from exclusion plots of the BNL E 734 [40], BNL E 776 [23] and CCFR [3]  $\nu_e \rightarrow \nu_e$  appearance experiments and of the FNAL E 531 [41] and CCFR [7]  $\nu_e \rightarrow \nu_e$  appearance experiments:

$$|A_{\nu\mu}| \leq |A_{\nu\mu}^0|; \quad (3.19)$$

with  $\nu = \mu$  and  $\nu = e; \mu$ . The results of the LSND [1]  $\nu_e \rightarrow \nu_e$  appearance experiment will be also taken into account (in particular, the allowed range (1.4) of  $m^2$ ).

Since scheme B emerges from scheme A by the substitution (3.9) and since we will derive bounds on the LBL oscillation probabilities  $P_{\nu\mu}^{(LBL;A)}$ ,  $P_{\nu\mu}^{(LBL;B)}$  and on the CP-odd parameters  $I^{(A)}$ ,  $I^{(B)}$  as functions of  $A_{\nu\mu}$ ,  $c$  and  $c$ , it is evident that such bounds apply equally to both schemes A and B by virtue of the definitions (3.4), (3.15) and (3.16). Consequently, when dealing with such bounds we will omit the superscripts A, B indicating the specific scheme.

#### IV. CONSTRAINTS ON THE LONG-BASELINE PROBABILITIES

We will consider first the limits on the LBL oscillation probabilities which can be obtained from the results of the SBL oscillation experiments. The Cauchy-Schwarz inequality implies for scheme A that

$$\sum_{k=1,2} |U_{\nu k}|^2 |U_{\mu k}|^2 \exp \left( -\frac{m_{k1}^2 L}{2p} \right) \leq c^2; \quad (4.1)$$

Using this inequality and the definition (3.15) of  $c$ , we find from the LBL probabilities in Eqs.(3.7) and (3.8) that the survival probabilities  $P_{\nu\nu}^{(LBL)}$  and  $P_{\nu\nu}^{(LBL)}$  are bounded by

$$(1 - c)^2 \leq P_{\nu\nu}^{(LBL)} \leq c^2 + (1 - c)^2; \quad (4.2)$$

As explained at the end of the last section, these bounds are scheme-independent. In order to obtain bounds on the LBL transition probabilities  $P_{\nu\mu}^{(LBL)}$  and  $P_{\nu\mu}^{(LBL)}$ , we take into account

the definition (3.4) of  $A_{\alpha\beta}$  and the inequality (4.1). When inserted into Eqs.(3.7) and (3.8) they imply

$$\frac{1}{4} A_{\alpha\beta} \leq P_{\nu_e \nu_e}^{(LBL)} \leq c_e + \frac{1}{4} A_{\alpha\beta} \quad ; \quad (4.3)$$

The bounds (4.2) and (4.3) are the basis of the following considerations for the different oscillation channels in LBL experiments.

The smallness of  $c_e$  (see Eq.(3.17)) implies that the electron neutrino has a small mixing with the neutrinos whose mass-squared difference is responsible for the oscillations of atmospheric and LBL neutrinos ( $\nu_1, \nu_2$  in scheme A and  $\nu_3, \nu_4$  in scheme B). Hence, the probability of transitions of atmospheric and LBL electron neutrinos into other states is suppressed. Indeed, taking into account the constraint  $c_e \leq \frac{1}{4} A_{\alpha\beta}$ , the lower bound on  $P_{\nu_e \nu_e}^{(LBL)}$  and the upper bounds on  $P_{\nu_e \nu_e}^{(LBL)}$  which we will derive are rather strict.

Let us discuss first the bounds on the LBL survival probability  $P_{\nu_e \nu_e}^{(LBL)}$ . We will compare these bounds with the expected sensitivity of the CHOOZ [8] and Palo Verde [9] LBL reactor experiments. Taking into account the constraint (3.17) on  $c_e$ , Eq.(4.2) implies that in both schemes A and B

$$1 - P_{\nu_e \nu_e}^{(LBL)} \leq \frac{1}{4} A_{\alpha\beta} \quad ; \quad (4.4)$$

The curve corresponding to this limit obtained from the 90% CL exclusion plot of the Bugey [22] experiment is shown in Fig.1 (solid line). The expected sensitivities of the LBL reactor neutrino experiments CHOOZ and Palo Verde are also shown in Fig.1 as the dash-dotted and dash-dot-dotted vertical lines, respectively. These expected sensitivities with respect to  $1 - P_{\nu_e \nu_e}^{(LBL)}$  have been extracted by us from the figures presented in Refs. [8,9] showing the sensitivity of the respective experiments in the  $\sin^2 2\theta - \Delta m^2$  plane, using the fact that for high values of  $\Delta m^2$  each experiment is sensitive only to the averaged survival probability  $P_{\nu_e \nu_e}^{(LBL)} = \frac{1}{2} \sin^2 2\theta$ . Thus, the vertical lines in Fig.1 correspond to  $\frac{1}{2} \sin^2 2\theta$  at high  $\Delta m^2$ .

Figure 1 shows that, in the framework of the two schemes (3.1) with four neutrinos, which allow to accommodate all the indications in favour of neutrino oscillations, the existing data put rather strong limitations on the probability of LBL transitions of  $\nu_e$  into other states (for  $\Delta m^2 \lesssim 3 \text{ eV}^2$  the upper bound for  $1 - P_{\nu_e \nu_e}^{(LBL)}$  is close to the border of the region of sensitivity of the CHOOZ experiment, whereas for  $\Delta m^2 \gtrsim 3 \text{ eV}^2$  it is much smaller).

The shadowed region in Fig.1 corresponds to the range (1.4) of  $\Delta m^2$  allowed at 90% CL by the results of the LSND and all the other SBL experiments. It can be seen that the LSND signal indicates an upper bound for  $1 - P_{\nu_e \nu_e}^{(LBL)}$  of about  $5 \cdot 10^{-2}$ , smaller than the expected sensitivities of the CHOOZ and Palo Verde experiments.

Let us stress that, in the framework of the schemes under consideration, the smallness of  $c_e$  is a consequence of the solar neutrino problem. Consider for example scheme A. The probability of solar neutrinos to survive is given by

$$P_{\nu_e \nu_e}^{(solar A)} = \sum_{k=1,2} |U_{ek}|^4 + \sum_{k=1,2} |U_{ek}|^2 P_{\nu_e \nu_e}^{(3,4)} \quad ; \quad (4.5)$$

where  $P_{e\mu}^{(3;4)}$  is the survival probability due to the mixing of  $\nu_e$  with  $\nu_3$  and  $\nu_4$ , depending on the small mass-squared difference  $\Delta m_{43}^2$ . From the results of SBL reactor experiments it follows that the quantity  $c_e = \sum_{k=1;2} J_{ek}^2$  can be small or large (close to one). In order

to have the energy dependence of the survival probability  $P_{e\mu}^{(\text{sun};A)}$  and the suppression of the flux of solar  $\nu_e$ 's that are required for the explanation of the data of solar neutrino experiments, we must choose a small value of  $c_e$ . In this case, the survival probability of  $\nu_e$ 's in LBL reactor experiments is close to one.

Let us now discuss the bounds on  $\nu_e \rightarrow \nu_\mu$  transitions in LBL accelerator experiments. We will compare these bounds with the expected sensitivities of the KEK {Super-Kamiokande (KEK {SK) [10], Fermilab {Soudan (MINOS) [11] and CERN {Gran Sasso (ICARUS) [12] experiments.

Taking into account the constraints (3.17) on  $c_e$  and (3.19) on  $A_{\nu_e}$ , Eq.(4.3) implies that in both schemes A and B

$$P_{(\nu_e) \rightarrow (\nu_\mu)}^{(\text{LBL})} \leq a_e^0 + \frac{1}{4} A_{\nu_e}^0 : \quad (4.6)$$

The curve corresponding to this limit obtained from the 90% CL exclusion plots of the Bugey [22] experiment for  $a_e^0$  and of the BNL E734 [40], BNL E776 [23] and CCFR [7] experiments for  $A_{\nu_e}^0$  is shown in Fig.2 (long-dashed line). For a comparison, we have shown the expected sensitivities of the LBL accelerator neutrino experiments KEK {SK [10], MINOS [11] and ICARUS [12] (the dotted, dash-dotted and dash-dot-dotted vertical lines, respectively). These sensitivities have been obtained from the figures presented in Refs. [10-12] showing the sensitivities of the respective experiments in the  $\sin^2 2\theta$  vs  $\Delta m^2$  plane with the method explained in the context of LBL reactor experiments.

The conservation of probability and Eq.(4.2) lead to a further upper bound:

$$P_{\nu_e \rightarrow \nu_\mu}^{(\text{LBL})} \leq 1 - P_{\nu_\mu \rightarrow \nu_e}^{(\text{LBL})} \approx c(2 - c) \quad (\epsilon) : \quad (4.7)$$

CPT invariance (see Eq.(2.4)) and the fact that the bound (4.2) is valid for antineutrinos as well give the same upper bound as Eq.(4.7) for the opposite transition  $\bar{\nu}_\mu \rightarrow \bar{\nu}_e$ :

$$P_{\bar{\nu}_\mu \rightarrow \bar{\nu}_e}^{(\text{LBL})} = P_{\nu_e \rightarrow \nu_\mu}^{(\text{LBL})} \leq 1 - P_{\nu_\mu \rightarrow \nu_e}^{(\text{LBL})} \approx c(2 - c) \quad (\epsilon) : \quad (4.8)$$

Finally, these two equations hold evidently also for antineutrinos. The solid curve in Fig.2 represents the limit

$$P_{(\bar{\nu}_\mu) \rightarrow (\bar{\nu}_e)}^{(\text{LBL})} \leq a_e^0 - 2 a_e^0 \quad (4.9)$$

obtained from Eq.(4.8) and the constraint (3.17) on  $c_e$ . This bound is better than the bound (4.6) for the SBL parameter  $\Delta m^2 \leq 0.4 \text{ eV}^2$ .

The darkly shadowed area in Fig.2 represents the region allowed by the results of the LSND [1] experiment, taking into account the results of all the other SBL experiments. The lower bound on  $P_{(\bar{\nu}_\mu) \rightarrow (\bar{\nu}_e)}^{(\text{LBL})}$ , i.e. the left edge of the shadowed region, is determined by the results

of the LSND experiment, whereas the upper bound is given by the limits obtained before, i.e. by the most stringent of the inequalities (4.9) and (4.6) represented, respectively, by the solid and long-dashed curves. Thus, for each fixed value of  $m^2$  we have

$$\frac{1}{4} A_{\nu e}^{m \text{ in}} \leq P_{(\nu) \nu_e}^{(\text{LBL})} \leq m \text{ in } a_e^0 \leq 2 a_e^0 ; a_e^0 + \frac{1}{4} A_{\nu e}^0 ; \quad (4.10)$$

where  $A_{\nu e}^{m \text{ in}}$  is the minimal value of  $A_{\nu e}$  allowed at 90% CL by the LSND experiment.

Figure 2 shows that, in the framework of the schemes under consideration, the sensitivity of the KEK (SK) experiment may be not sufficient to reveal LBL  $\nu_e$  oscillations, whereas the sensitivities of the MINOS and ICARUS experiments are considerably better than the upper bound for  $P_{(\nu) \nu_e}^{(\text{LBL})}$ . It is interesting to observe that there is also a lower bound on this transition probability that follows from the LSND results (see Eq.(4.10)). However, this lower bound is valid only in the case of LBL neutrino oscillations in vacuum. The corrections due to the matter effects in LBL experiments make it disappear (see Section V II).

The solid curve in Fig 2 is at the same time an upper bound on  $P_{(\nu) \nu_e}^{(\text{LBL})}$ . This is evident from Eq.(4.7). On the other hand, the probability of  $(\nu) \nu_e$  transitions is not constrained by the results of SBL experiments.

Finally, a further upper bound on  $P_{(\nu) \nu_e}^{(\text{LBL})}$  for  $\nu_e$  is gained from Eq.(4.3). Since  $A_{\nu e} \leq 4(1-c)(1-c)$ , we have

$$P_{(\nu) \nu_e}^{(\text{LBL})} \leq c c + (1-c)(1-c) \quad (\nu_e) : \quad (4.11)$$

Obviously, if  $c = c = 0$  or  $1$  is in the allowed range of these quantities, then this upper bound is  $1$  and thus is trivial. This leaves only  $c = 0$  and  $c = 1$  as a non-trivial case, with

$$P_{(\nu) \nu_e}^{(\text{LBL})} \leq a_e^0 + a^0 \leq 2 a_e^0 a^0 : \quad (4.12)$$

The short-dashed curve in Fig 2 shows this limit with  $a_e^0$  and  $a^0$  obtained from the 90% CL exclusion plots of the Bugey [22]  $\nu_e$  experiment and of the CDHS [37] and CCFR [38]  $\nu_e$  experiments, respectively. For  $a^0 \leq a_e^0 \leq 1$  this bound is about half of that given by Eq.(4.9). However, since  $a^0$  is only small in the same range of  $m^2$  where  $A_{\nu e}^0$  is small, numerically the bound (4.12) turns out to be worse than the bound (4.6) (the long-dashed curve in Fig 2).

## V. CP VIOLATION IN THE SCHEMES WITH FOUR NEUTRINOS

As shown in Appendix B, the unitarity of the mixing matrix implies the "unitarity bound"

$$\sum_j |U_{ij}|^2 = f(x; y) \quad (5.1)$$

where  $f(x; y)$  is the continuous function

$$f(x;y) = \begin{cases} f_1 - xy & \text{for } 2(1-x)(1-y) \geq xy \\ f_2 - 2[(x+y-1)(1-x)(1-y)] & \text{for } 2(1-x)(1-y) < xy \end{cases} \quad (5.2)$$

defined on the unit square  $0 \leq x \leq 1, 0 \leq y \leq 1$ . In Fig.3 we have drawn a contour plot of the function  $f(x;y)$ , which is helpful for the determination of the maximal allowed value for  $f(c_e; c_e)$  when  $c_e$  and/or  $c_e$  are bounded. The dotted line in Fig.3 is the borderline  $g(x) = 2(1-x) = 2-x$  between the regions where  $f = f_1$  and  $f = f_2$ . Note that  $f$  is continuous along this borderline.

In order to determine the maximum of  $f(x;y)$ , the following considerations are useful (for the details consult Appendix C). Increasing  $x$  at fixed  $y$ , the function  $f$  increases monotonously from  $f = 0$  at  $x = 0$ , until the straight line  $y_1(x) = 2 \frac{2x}{1-x} (1=2-x)$  depicted in Fig.3 is reached. There, the value of  $f$  is given by  $f = \frac{y}{1-x}$ . After this intersection, the function  $f$  decreases monotonously to  $f = 0$  at  $x = 1$ . From the symmetry  $f(x;y) = f(y;x)$ , it follows that for fixed  $x$  and increasing  $y$  the function  $f$  increases monotonously from  $f = 0$  at  $y = 0$  to  $f = \frac{x}{1-y}$  when the straight line  $y_2(x) = 1-x = 2(0 \leq x \leq 1)$  depicted in Fig.3 is crossed. After this intersection,  $f$  decreases monotonously to  $f = 0$  at  $y = 1$ .

The absolute maximum of the function  $f$  (see Appendix C) lies at the intersection of the lines  $y_1$  and  $y_2$  and is given by  $f_{max} = 2 - \sqrt{3} \approx 0.385$ . Therefore, from the unitarity of the mixing matrix we have an absolute maximum for  $J_{e j}$ :

$$J_{e j} \leq \frac{2}{3^{3/2}} \approx 0.385 \quad (5.3)$$

With the help of Fig.3, one can see that Eq.(5.1) with the constraints (3.17) on  $c_e$  and  $c_e$  implies that

$$J_{e j} < \begin{cases} f_2(a_e^0; y_2(a_e^0)) = a_e^0 \frac{1}{1-a_e^0} & \text{for } a_e^0 \leq \frac{1}{2} \\ f_2(a_e^0; 1-a_e^0) = 2 a_e^0 (1-a_e^0) & \text{for } a_e^0 > \frac{1}{2} \end{cases} \quad (5.4)$$

The solid curve in Fig.4 shows the limit  $J_{e j} \leq \frac{1}{1-a_e^0}$  with  $a_e^0$  obtained from the 90% CL exclusion plot of the Bugey [22]  $\nu_e - \nu_e$  experiment. The dotted curve in Fig.4 represents the improvement reached with the lower part of Eq.(5.4) at the values of  $m^2$  for which  $a_e^0 \leq \frac{1}{2}$ , with  $a_e^0$  obtained from the 90% CL exclusion plots of the CDHS [37] and CCFR [38]  $\nu_e - \nu_e$  experiments.

The bound represented by the solid curve in Fig.4 is valid also for  $J_{e j}$  because there is no experimental information on  $c_e$ .

For  $J_{e j}$  again by inspection of Fig.3, one can see that Eq.(5.1) with the constraints (3.17) on  $c_e$  implies that

$$J_{e j} \leq \frac{1}{1-a_e^0}; y_2(1-a_e^0) = \frac{1-a_e^0}{1-a_e^0} \quad (5.5)$$

The solid curve in Fig.5 represents the corresponding bound obtained from the 90% CL exclusion curves of the CDHS [37] and CCFR [38]  $\nu_e - \nu_e$  experiments. For  $m^2 \leq 0.3 \text{ eV}^2$  there are no experimental data and therefore  $J_{e j} \leq 0.385$  by virtue of Eq.(5.3).

Taking into account the expression (3.4) for  $A_{ij}$ , in both schemes A and B we have (for the proof of this inequality, see Appendix A)

$$|J_{ij}| < \frac{1}{2} \sqrt{A_{ij}^0 (4c_{ij}^2 - A_{ij}^0)} \quad (5.6)$$

Taking into account Eq.(3.19), we obtain

$$|J_{ij}| < \begin{cases} \frac{1}{2} \sqrt{A_{ij}^0 (4c_{ij}^2 - A_{ij}^0)} & \text{for } A_{ij}^0 > 2c_{ij}^2 \\ c_{ij}^2 & \text{for } A_{ij}^0 < 2c_{ij}^2 \end{cases} \quad (5.7)$$

For  $J_{e\mu}$  with the constraints (3.17), the inequality (5.7) becomes

$$|J_{e\mu}| < \begin{cases} \frac{1}{2} \sqrt{A_{e\mu}^0 (4a_e^0 - A_{e\mu}^0)} & \text{for } A_{e\mu}^0 > 2a_e^0 \\ a_e^0 & \text{for } A_{e\mu}^0 < 2a_e^0 \end{cases} \quad (5.8)$$

The dash-dotted curve in Fig.4 shows the limit (5.8) obtained using the 90% exclusion plots of the Bugey [22]  $\nu_e \rightarrow \nu_\mu$  experiment for the determination of  $a_e^0$  and the BNL E734 [40], BNL E776 [23] and CCFR [3]  $\nu_e \rightarrow \nu_\mu$  experiments for the determination of  $A_{e\mu}^0$ .

Since the constraints (3.17) do not put an upper bound on the possible values of  $c_{ij}$  and  $c_{\mu j}$ , in the case of  $|J_{ij}|$  the inequality (5.7) becomes

$$|J_{ij}| < \frac{1}{2} \sqrt{A_{ij}^0 (4 - A_{ij}^0)} \quad (5.9)$$

The dotted curve in Fig.5 shows the limit (5.9) obtained using the 90% exclusion plot of the FNAL E531 [41] and CCFR [7]  $\nu_\mu \rightarrow \nu_\tau$  experiment for the determination of  $A_{ij}^0$ .

The shadowed regions in Figs.4 and 5 correspond to the range (1.4) of  $m^2$  allowed at 90% CL by the results of the LSND and all the other SBL experiments. From Fig.5 it can be seen that, taking into account the LSND signal,  $|J_{ij}|$  could be close to the maximal value  $2/3$  allowed by the unitarity of the mixing matrix.

## VI. THREE MASSIVE NEUTRINOS

It is worthwhile to have a look at LBL neutrino oscillation experiments neglecting some of the present hints for neutrino oscillations. It is possible that not all these hints will be substantiated in the course of time and it is useful to check which features are actually dependent on or independent from them.

In this Section we consider the minimal scenario of mixing of three neutrinos. We will assume that of the two differences of neutrino mass-squared one is relevant for SBL oscillations and the other one for LBL oscillations (see also Refs. [26,28]). Hence, in this section we adopt the point of view that not neutrino mixing but other reasons could explain the solar neutrino data. With these assumptions, there are two possible three-neutrino mass spectra:

$$(I) \quad \underbrace{m_1 < m_2 < m_3}_{\text{SBL}} \quad \text{and} \quad (II) \quad \underbrace{m_1 < m_3 < m_2}_{\text{SBL}} ; \quad (6.1)$$

In both schemes I and II,  $m_{31}^2$  is assumed to be relevant for neutrino oscillations in SBL experiments. In this case, the SBL oscillation probabilities depend on  $\theta_{e3}$  and  $\theta_{31}$  in the scheme I [39] and on  $\theta_{e1}$  and  $\theta_{13}$  in the scheme II [36]. There are three regions of these quantities which are allowed by the results of disappearance experiments (see Refs. [39,36]):

$$\begin{aligned} (1) \quad & \theta_{ek} \neq 0; \quad \theta_{kj} = 0; \\ (2) \quad & \theta_{ek} = 0; \quad \theta_{kj} = 0; \\ (3) \quad & \theta_{ek} = 0; \quad \theta_{kj} = \pi; \end{aligned} \quad (6.2)$$

with  $k = 3$  for the scheme I and  $k = 1$  for the scheme II<sup>2</sup> (for the definition of  $a_e^0$  and  $a^0$ , see Eq.(3.18)).

The neutrino and antineutrino LBL oscillation probabilities in scheme I are given by

$$P_{\nu}^{(LBL;I)} = U_{11}U_{11} + U_{21}U_{21} \exp\left[-\frac{m_{21}^2 L}{2p}\right]^2 + \theta_{31}\theta_{31}; \quad (6.3)$$

$$P_{\bar{\nu}}^{(LBL;I)} = U_{11}U_{11} + U_{21}U_{21} \exp\left[-\frac{m_{21}^2 L}{2p}\right]^2 + \theta_{31}\theta_{31}; \quad (6.4)$$

From the comparison of Eqs.(6.3) and (6.4) with Eqs.(3.7) and (3.8), it is obvious that the CP-odd asymmetries  $D_{\nu}^{(LBL;I)}$  are given by the same formula (3.10) as in the 4-neutrino case (with  $I^{(A)} \rightarrow I^{(I)}$ ). The transition probabilities in the scheme II can be obtained from the expressions (6.3) and (6.4) with the cyclic permutation of the indices

$$1;2;3 \rightarrow 2;3;1; \quad (6.5)$$

Therefore, as in the case of the schemes A and B for four neutrinos, the bounds on the LBL oscillation probabilities and the CP-odd asymmetries are the same in the three neutrino schemes I and II.

The bounds on the LBL oscillation probabilities  $P_{\nu}^{(LBL)}$  and on the CP-odd parameters  $I$  derived in the Appendices for the four-neutrino schemes (3.1) are valid also in the case of mixing of three neutrinos: the demonstrations in the four-neutrino case A (B) can be applied to the three neutrino case I (II) if we put  $U_{41} = 0$  ( $U_{14} = 0$ ) and change the indices  $2;3;4 \rightarrow 1;2;3$  for all  $\nu = e, \mu, \tau$ .

<sup>2</sup> For a comparison, the schemes I, II and the regions 1, 2, 3 are called hierarchies II, I and regions A, B, C, respectively, in Ref. [26].

It is obvious that, with  $A_{\mu\nu} = 4J_{31}J_{32}J_{33}$ , the same bounds on  $P_{(\mu)(\nu)}^{(LBL)}$  arise for  $\mu = \nu$  and  $\mu \neq \nu$  as given by Eqs.(4.2) and (4.3). Since in the 3-neutrino case the CP-odd asymmetries in different oscillation channels are connected by Eq.(2.11), we have

$$I_e = I_{\mu} = I_{\nu} : \quad (6.6)$$

A few remarks on the unitarity bound (5.1) are in order. It is true that from the unitarity of the  $3 \times 3$  mixing matrix we have  $A_{\mu\nu} = 4(1 - c_{\mu})(1 - c_{\nu})$  and  $c_{\mu} + c_{\nu} = 1$ , but, nevertheless, the distinction defined by Eq.(6.6) has to be maintained. Therefore, also the unitarity bound is upheld with the addendum that  $c_{\mu}$  and  $c_{\nu}$  can only vary within the section of the unit square defined by  $c_{\mu} + c_{\nu} = 1$ . Since the point  $c_{\mu} = c_{\nu} = 2/3$  fulfills this condition, the absolute maximum  $|J_{\mu\nu}|_{\text{max}} = 2/3\sqrt{3}$  of the 4-neutrino case extends its validity to three neutrinos<sup>3</sup>.

In the following we will give LBL bounds for each of the regions (6.2), along the lines of the previous 4-neutrino sections.

Region 1. With respect to SBL and LBL neutrino oscillations, the 3-neutrino schemes I and II in Region 1 correspond to the 4-neutrino schemes A and B, respectively, with the same bounds on  $P_{(\mu)(\nu)}^{(LBL)}$  (Eq.(4.4) and Fig.1),  $P_{(\mu)(\nu)}^{(LBL)}$  (Eqs.(4.6), (4.9), (4.12) and Fig.2) and  $J_{\mu\nu}$  (Eqs.(5.4), (5.8) and Fig.4). Since  $|J_{\mu\nu}| = |J_{\nu\mu}|$  the stringent bounds on  $J_{\mu\nu}$  given in Fig.4 are valid also for  $J_{\nu\mu}$ .

For completeness, we want to mention that there is a change in the upper bound for  $P_{(\mu)(\nu)}^{(LBL)}$  in going from four to three neutrinos: taking into account the inequality  $c_e + c_{\mu} = 1$ , we have  $c_{\mu} = 1 - m$  in  $(\mu; a^0)$  and Eq.(4.12) improves to

$$P_{(\mu)(\nu)}^{(LBL)} \leq a_e^0 + (1 - 2a_e^0)m \text{ in } (a_e^0; a^0) : \quad (6.7)$$

For  $a_e^0 < a^0$  this bound is slightly more stringent than that given by Eq.(4.9), but the improvement is negligible for  $a_e^0 \approx 1$ .

Region 2. Actually, this Region is excluded by the results of the LSND experiment (see Refs. [39,36,24]). The reason is that (in combination with other data) the upper bound

$$A_{\mu\nu} \approx 4a_e^0 a^0 \quad (6.8)$$

is too restrictive to be compatible with the LSND data. In spite of this evidence, let us discuss the bounds on the LBL probabilities in this Region.

The restrictions  $c_e = 1 - a_e^0$ ,  $c_{\mu} = 1 - a^0$  and the unitarity of the mixing matrix imply that  $c_{\nu}$  is small:  $c_{\nu} = 2 - c_e - c_{\mu} = a_e^0 + a^0$ . From Eq.(4.3) it follows that the probabilities of  $(\mu)(\nu)$  and  $(\nu)(\mu)$  transitions in LBL experiments are confined in the range

---

<sup>3</sup>This value is 4 times the maximal value of the Jarlskog parameter  $J$  [42] for CP violation in the Kobayashi-Maskawa matrix,  $|J|_{\text{max}} = 1/6\sqrt{3}$ .

$$\frac{1}{4}A; \quad P_{(\ )!(\ )}^{(LBL)} = \frac{1}{4}A; + a_e^0 + a^0 \quad (= e; ); \quad (6.9)$$

whereas for the probability of  $(\ )!(\ )_e$  transitions we have only the lower bound

$$\frac{1}{4}A_{e; } \leq P_{(\ )!(\ )_e}^{(LBL)}; \quad (6.10)$$

The inequality (4.8) yields the additional upper bounds

$$P_{(\ )!(\ )}^{(LBL)} \leq a_e^0 + a^0 \leq 2 \quad a_e^0 \quad a^0 \quad (= e; ); \quad (6.11)$$

The bounds on CP violation can be derived with the methods described in the Appendices. They are given by the oscillation amplitude bound

$$j_{e; j} \leq \frac{1}{2} \sqrt{\frac{A_{e; }^0}{4} - A_{e; }^0}; \quad (6.12)$$

and the unitarity bound

$$j_{e; j} \leq \sqrt{1 - a_e^0} \quad a^0 = 2 \sqrt{a_e^0 a^0 - 1} \quad a_e^0 \quad a^0; \quad (6.13)$$

Both are of similar order of magnitude and less restrictive than the bounds in Region 1. Since  $j_{\bar{l} j} = j_{e; j}$ , these bounds are valid also for  $j_{\bar{l} j}$ .

Region 3. In this Region, where  $c_e \leq 1 - \frac{a}{2}$  and  $c \leq a$ , the atmospheric neutrino data cannot be explained in the framework discussed here. The reason is that

$$P_{(\ )!(\ )}^{(LBL)} \leq (1 - \frac{a}{2})^2 \quad (6.14)$$

and this is incompatible [24] with the atmospheric neutrino anomaly. The LBL transition probabilities of muon neutrinos are connected by

$$\frac{1}{4}A; \quad P_{(\ )!(\ )}^{(LBL)} = \frac{1}{4}A; + a^0 \quad (= e; ); \quad (6.15)$$

whereas for  $(\ )!(\ )_e$  transitions there is only the lower bound

$$\frac{1}{4}A_{e; } \leq P_{(\ )!(\ )_e}^{(LBL)}; \quad (6.16)$$

The inequality (4.7), which is a consequence of probability conservation, leads to

$$P_{(\ )!(\ )}^{(LBL)} \leq a^0 \leq 2 \quad a^0 \quad (= e; ); \quad (6.17)$$

Furthermore, taking into account the inequality  $c_e + c \leq 1$ , we have  $c_e \leq 1 - m$  in  $(\frac{a}{2}; a^0)$  and Eq.(4.12) improves to

$$P_{e \rightarrow e}^{(LBL)} = a^0 + (1 - 2a^0) \min(a_e^0; a^0) : \quad (6.18)$$

For  $a_e^0 = a^0 = 1$  this bound is about half of that given by Eq.(6.17).

Finally, our methods for obtaining bounds on CP violation yield

$$|\mathcal{J}_e| \leq \frac{1}{2} \sqrt{A_{\nu e}^0 - 4a^0 A_{\nu e}^0} \quad (6.19)$$

and

$$|\mathcal{J}_e| \leq \begin{cases} a^0 - 1 & \text{for } a_e^0 = a^0 = 2; \\ 2 - a^0 & \text{for } a_e^0 = a^0 = 2; \end{cases} \quad (6.20)$$

The oscillation amplitude bound is more stringent in this case. From Eq.(6.6) it follows that the bounds (6.19) and (6.20) are valid also for the parameter  $|\mathcal{J}|$  that characterizes the CP-odd asymmetry in the  $\mu$  channel.

The differences in the bounds on the LBL probabilities are marked and could thus serve to distinguish between the three different Regions in the three neutrino case. Of course, in the experiments discussed here the four neutrino case (schemes A and B) is indistinguishable from the three neutrino case with Region 1. The above-mentioned distinctions could also serve as a cross-check for present hints of neutrino oscillations.

## VII. CONCLUSIONS

At present there are three experimental indications in favour of neutrino oscillations which correspond to three different scales of neutrino mass-squared differences: the solar neutrino deficit, the atmospheric neutrino anomaly and the result of the LSND experiment. These indications and the negative results of numerous short-baseline neutrino experiments can be accommodated in two schemes (A and B) with mixing of four massive neutrinos [24]. In this paper we have presented a detailed study of the predictions of the schemes A and B for long-baseline experiments. Using only the results of existing experiments, we have obtained bounds on probabilities of different transitions in long-baseline experiments.

The schemes A and B give completely different predictions for neutrinoless double beta decay and for neutrino mass effects in experiments for neutrino mass measurements by the tritium method [24]. They lead, however, to the same bounds on long-baseline oscillation probabilities. In addition, all the bounds that we have derived apply for neutrinos as well as antineutrinos.

We have shown that the results of the short-baseline reactor experiment put rather severe bounds on the probability  $1 - P_{e \rightarrow e}^{(LBL)}$  of  $e$  transitions into all possible other states in long-baseline experiments. If the  $m^2$  relevant in short-baseline oscillations is bigger than about  $3 \text{ eV}^2$ , the bound on  $1 - P_{e \rightarrow e}^{(LBL)}$  is slightly higher than the sensitivity of the CHOOZ experiment, allowing some possibility to reveal neutrino oscillations in this channel. However, the results of the LSND experiment favour the range  $0.3 \leq m^2 \leq 2.2 \text{ eV}^2$ . We have shown that in this range the upper bound for the quantity  $1 - P_{e \rightarrow e}^{(LBL)}$  lies between  $10^{-2}$

and  $5 \cdot 10^2$  (see Fig.1) and thus below the sensitivity of CHOOZ and Palo Verde. On the other hand, there is no restriction on  $P_{(\nu_e) \rightarrow (\nu_e)}^{(LBL)}$ .

The probability  $P_{(\nu_e) \rightarrow (\nu_e)}^{(LBL)}$  of  $(\nu_e) \rightarrow (\nu_e)$  transitions is severely constrained in the schemes A and B by the results of short-baseline reactor and accelerator experiments (see Fig.2). The sensitivity of MINOS and ICARUS is well below the upper bound for  $P_{(\nu_e) \rightarrow (\nu_e)}^{(LBL)}$ , whereas the sensitivity of the KEK-SK experiment seems to be insufficient. There is also an upper bound on long-baseline  $(\nu_e) \rightarrow (\nu_e)$  oscillations (solid curve in Fig.2), which is nearly as tight as the one for  $(\nu_e) \rightarrow (\nu_e)$  transitions. On the other hand, the long-baseline  $(\nu_e) \rightarrow (\nu_e)$  channel is unconstrained.

We have obtained bounds on LBL transition probabilities in the case of the neutrino mass spectra (3.1), which are implied by the results of the solar, atmospheric and LSND experiments. If the LSND data are not confirmed by future experiments, but nevertheless there is a mass (or masses) approximately equal to 1 eV providing an explanation for the hot dark matter problem, then the neutrino mass spectrum can be different from the spectra A and B in Eq.(3.1). The natural neutrino mass spectrum in this case is hierarchical and in this case the bounds that we have obtained in this paper are not valid.

In the framework of neutrino mixing in schemes A and B, we have also derived constraints on the parameters  $I_{\mu\nu}$  that characterize the CP-odd neutrino{antineutrino} asymmetries in long-baseline experiments. We have developed methods for deriving upper bounds on the parameters  $I_{\mu\nu}$  from the data of short-baseline experiments, which can be applied to different schemes. We have shown that CP violation in the  $(\nu_e) \rightarrow (\nu_e)$  channel is bounded by  $|I_{e\bar{e}}| \cdot 10^2$ . A similar suppression of CP-odd effect takes place in  $(\nu_e) \rightarrow (\nu_e)$  long-baseline neutrino oscillations. On the other hand, sizable CP violation can be expected in  $(\nu_e) \rightarrow (\nu_e)$  oscillations. The CP-odd asymmetry in this channel could be close to its maximally allowed value  $|I_{\mu\nu}|_{\max} = 0.385$ , resulting from unitarity of the mixing matrix.

Summarizing, we would like to emphasize that the results of all neutrino oscillation experiments lead to severe constraints on the probabilities for the probabilities for  $(\nu_e)$  disappearance and  $(\nu_e) \rightarrow (\nu_e)$  and  $(\nu_e) \rightarrow (\nu_e)$  appearance in long-baseline experiments. Nevertheless, even these channels are within the planned sensitivity of the MINOS and ICARUS experiments. The channels  $(\nu_e) \rightarrow (\nu_e)$  and  $(\nu_e) \rightarrow (\nu_e)$  are not constrained at all. Therefore, from the point of view of the present investigation, long-baseline muon neutrino beams provide promising facilities for the observation of neutrino oscillations.

Let us stress that we have considered here vacuum LBL oscillations. In conclusion, we want to present some remarks about the effects of matter. In the 4-neutrino schemes under consideration active neutrinos can transform into sterile states. Therefore, not only charged current but also neutral current interactions must be taken into account [16] and the effective Hamiltonian in the flavour representation is given by

$$H_e = \frac{1}{2p} U M^2 U^\dagger + \text{diag} (a_{CC}; 0; 0; a_{NC}) \quad (7.1)$$

with

$$a_{CC} = 2 \frac{p}{2} G_F N_e p' \approx 8 \cdot 10^5 \text{ eV}^2 \frac{p}{1 \text{ g cm}^{-3}} \frac{p}{1 \text{ GeV}} ; \quad (7.2)$$

$$a_{N_C} = \frac{p}{2} G_F N_n p' \frac{1}{2} a_{C_C} \quad (7.3)$$

where  $\hat{M}^2$  is the diagonal matrix of the squared masses,  $G_F$  is the Fermi constant,  $N_e$  and  $N_n$  are the electron and neutron number density<sup>4</sup>, respectively, and  $\rho$  is the density of matter, which in the Earth's crust is of the order of  $3 \text{ g cm}^{-3}$ . The parameters  $a_{C_C}$  and  $a_{N_C}$  are small with respect to the  $m^2$  relevant for LBL oscillations. Nevertheless, their contributions for some transitions can be important (see [28] for the case of three neutrinos).

In order to take into account the matter effects in the oscillation probabilities we must diagonalize  $H_e$ <sup>5</sup>. In the case of the schemes (3.1) under consideration, the relation  $a_{C_C} = m^2 = 1 \text{ eV}^2$  is valid and thus, up to terms of the order  $a_{C_C} = m^2$ , we have

$$H_e = U^0 \hat{M}^2 U^{0\dagger} \quad (7.4)$$

where  $\hat{M}^2 = \text{diag}(m_1^2, \dots, m_4^2)$ ,  $U^0 = UR$  and  $R$  has the block structure

$$R = \begin{pmatrix} R^0 & 0 \\ 0 & R^{00} \end{pmatrix} : \quad (7.5)$$

The matrices  $R^0$  and  $R^{00}$  are  $2 \times 2$  unitary matrices. Now instead of Eq.(3.7) we obtain for the LBL oscillation probabilities

$$P_{\nu_e \rightarrow \nu_e}^{(LBL)} = \sum_{j=1,2} |U_j^0 U_j^0|^2 \exp\left(-\frac{m_j^2 L}{2p}\right) + \sum_{k=3,4} |U_k^0 U_k^0|^2 \exp\left(-\frac{m_k^2 L}{2p}\right) : \quad (7.6)$$

From the Cauchy-Schwarz inequality it is easy to see that in both schemes A and B the upper bounds (4.2), (4.11) and therefore (4.12) (represented by the short-dashed curve in Fig 2) are valid in the case of matter apart from corrections of the order of  $a_{C_C} = m^2$ . Other bounds could be modified by the matter effect.

However, the upper bound (4.4) applied to reactor LBL experiments is practically not modified by matter effects. In fact, the relevant parameter  $a_{C_C} L = 2p = 0.5 \cdot 10^6 (L=1 \text{ m})$ , for  $\rho = 3 \text{ g cm}^{-3}$ , is around  $10^4$  for CHOOZ and Palo Verde, whereas in the case of MINOS and ICARUS it is not small ( $a_{C_C} L = 2p = 0.4$ ). For the KEK-SK experiment, matter corrections are still modest because the baseline is roughly a factor of three smaller than the baseline of MINOS and ICARUS. Due to matter effects the bounds (4.6) and (4.9) on the  $\nu_e$  transition probability depicted in Fig 2 become less restrictive, in particular for the MINOS and ICARUS experiments. Note that also because matter induces corrections of the order of  $10^2$  the lower bound obtained in the vacuum case from the results of the LSND experiment (the left borderline of the darkly shadowed area in Fig 2) disappears and the lightly shadowed region in Fig 2 is allowed by the LSND experiment in the case of LBL

<sup>4</sup> $N_e = N_n = \frac{N_A}{2} \rho$ , where  $N_A$  is the Avogadro number.

<sup>5</sup> Here we consider the simplifying approximation of constant  $N_e$  and  $N_n$ .

oscillations in matter. A detailed discussion of matter effects in the case of mixing of four massive neutrinos will be published elsewhere [43].

For antineutrinos the relevant effective Hamiltonian is obtained from Eq.(7.1) by taking  $U^*$  instead of  $U$  and putting a minus in front of  $a_{CC}$  and  $a_{NC}$ . Therefore, matter effects can mimic CP-odd asymmetries and at least at the order of  $10^{-2}$  both effects are entangled. In the framework of the schemes with mixing of three neutrinos the effects of matter in long-baseline experiments were considered recently in Refs. [26-28]. It was shown that the contribution of matter to the CP-odd asymmetries is small for all transitions, except for  $\nu_e \rightarrow \bar{\nu}_e$  transitions in the Region 2 of the scheme I [28], which is not compatible with the LSND result [39].

#### ACKNOWLEDGMENTS

This work was done while one of authors (S.M.B.) was Lady Davis visiting professor at the Technion. This author would like to thank the Physics Department of Technion for its hospitality.

APPENDIX A : DERIVATION OF THE OSCILLATION AMPLITUDE BOUND

In this Appendix we discuss the derivation of the "oscillation amplitude bound". The starting point is the quantity

$$I = 4 \text{Im} U_{11} U_{12} U_{21} U_{22} \quad (6); \tag{A1}$$

which determines the CP-odd asymmetry in the case of four massive neutrinos.

It is obvious that  $I$  is invariant under the phase transformation

$$U_j \rightarrow e^{i\phi_j} U_j; \quad U_j \rightarrow e^{i\psi_j} U_j; \tag{A2}$$

where the  $\phi_j$  are arbitrary phases. Thus the elements  $U_j$  can be taken to be real. Taking into account the definitions (3.15) and (3.16) valid in the schemes A and B of Eq.(3.1), respectively, we can write

$$U_j = \frac{p_j}{c} e_j^{(1)}; \quad \text{with} \quad \begin{matrix} j=1;2 & \text{in the scheme A,} \\ j=3;4 & \text{in the scheme B,} \end{matrix} \tag{A3}$$

and the orthonormal basis

$$e^{(1)} = (\cos \theta; \sin \theta); \quad e^{(2)} = (\sin \theta; \cos \theta); \tag{A4}$$

We expand  $U_j$  (with  $j=1;2$  in the scheme A and  $j=3;4$  in the scheme B) with respect to this basis as

$$U_j = \frac{p_j}{c} \sum_{k=1,2} p_{kj} e_j^{(k)}; \tag{A5}$$

where  $p_1$  and  $p_2$  are complex coefficients such that

$$\sum_{k=1,2} |p_{kj}|^2 = 1; \tag{A6}$$

With the help of Eqs.(A3)-(A6) we easily find

$$I = 2 c^2 \sin 2\theta \text{Im}(p_1 p_2) = 2 c^2 \sum_{j=1,2} |p_{1j}|^2 \frac{p_1}{c} \frac{p_2}{c} \sin 2\theta \sin \phi_j; \tag{A7}$$

where  $\phi_j$  is the phase of  $p_1 p_2$ .

The parameter  $|p_{1j}|$  is connected to the oscillation amplitude  $A_j$ ; and the parameters  $c, \theta$ . In fact, from Eqs.(A3) and (A5) we have

$$A_j^2 = \sum_{k=1,2} \sum_{l=1,2} |U_{jk}|^2 |U_{lk}|^2 = \sum_{k=1,2} \sum_{l=1,2} \left( \frac{p_{kj}}{c} \right)^2 \left( \frac{p_{lk}}{c} \right)^2 \tag{A8}$$

in the scheme A ;

$$A_j^2 = \sum_{k=3,4} \sum_{l=3,4} |U_{jk}|^2 |U_{lk}|^2 = \sum_{k=3,4} \sum_{l=3,4} \left( \frac{p_{kj}}{c} \right)^2 \left( \frac{p_{lk}}{c} \right)^2$$

in the scheme B ;

Hence, in both schemes A and B, we have  $p_{1j} = \frac{p}{A_j} \sqrt{4c_1 c_2}$ . Inserting this value in Eq.(A 7), we obtain

$$I = \frac{1}{2} \sqrt{A_j (4c_1 c_2 - A_j)} \sin 2\theta_j \quad (A 9)$$

and thus we arrive at the "oscillation amplitude bound"

$$jI_j \leq \frac{1}{2} \sqrt{A_j (4c_1 c_2 - A_j)} \quad (A 10)$$

Let us stress that this derivation is based only on the obvious inequality

$$j \sin 2\theta_j \leq 1 \quad (A 11)$$

Since  $c_1, c_2$  and  $A_j$  do not restrict  $\theta_j$ , the bound (A 10) is the optimal one.

#### APPENDIX B: DERIVATION OF THE UNITARITY BOUND

Up to now we did not use the unitarity of the mixing matrix. Taking this fact into account will allow us to obtain an upper bound on  $jI_j$  depending solely on  $c_1$  and  $c_2$ .

The unitarity of the mixing matrix tells us that

$$\sum_{j=1;2} U_j U_j^\dagger = \sum_{j=3;4} U_j U_j^\dagger \quad (B 1)$$

This relation allows to write the oscillation amplitude  $A_j$  in the two forms of Eq.(3.4). Using the Cauchy-Schwarz inequality, one can see that

$$A_j = 4 \sum_{j=3;4} U_j U_j^\dagger \leq 4 \sum_{j=3;4} |U_j|^2 \sum_{j=3;4} |U_j|^2 = 4(1-c_1)(1-c_2); \quad (B 2)$$

in the scheme A, and

$$A_j = 4 \sum_{j=1;2} U_j U_j^\dagger \leq 4 \sum_{j=1;2} |U_j|^2 \sum_{j=1;2} |U_j|^2 = 4(1-c_1)(1-c_2); \quad (B 3)$$

in the scheme B. Hence, in both schemes A and B the oscillation amplitude  $A_j$  is bounded by

$$A_j \leq 4(1-c_1)(1-c_2) \quad (B 4)$$

The right-hand side of the inequality (A 10), as a function of  $A_j$ , reaches its maximum,  $c_1 c_2$ , at

$$(A_j)_0 = 2c_1 c_2 \quad (B 5)$$

Consequently, if the condition

$$2(1-c)(1-c) - c^2 \tag{B6}$$

is satisfied, the upper bound (B4) on  $A_{j,j}$  is larger than  $(A_{j,j})_0$ . In this case we have

$$A_{j,j} \geq c^2 \tag{B7}$$

If the condition (B6) is not fulfilled, the upper bound (B4) is smaller than  $(A_{j,j})_0$  and has to be inserted for  $A_{j,j}$  into Eq.(A10), leading to

$$A_{j,j} = \frac{c}{2(c+c-1)(1-c)(1-c)} \tag{B8}$$

Thus, we arrive at the "unitarity bound"

$$A_{j,j} = f(c;c) \tag{B9}$$

with the function

$$f(x;y) = \begin{cases} f_1 - xy & \text{for } 2(1-x)(1-y) \geq xy; \\ f_2 - 2[(x+y-1)(1-x)(1-y)]^2 & \text{for } 2(1-x)(1-y) < xy; \end{cases} \tag{B10}$$

defined on the unit square  $0 \leq x \leq 1, 0 \leq y \leq 1$ . The function

$$g(x) = \frac{2(1-x)}{2-x} \tag{B11}$$

represents the borderline separating the two regions in the definition of the function (B10). It is clear from our derivation (and also easy to check) that  $f$  is continuous along this borderline.

#### APPENDIX C : DISCUSSION OF THE FUNCTION $f$

Since we do not have definite experimental values of  $c_+$  and  $c_-$ , but only bounds on these quantities (see Eq.(3.17)), which define allowed rectangles in the square  $0 \leq c_+ \leq 1, 0 \leq c_- \leq 1$ , we are interested in the behaviour of  $f$  in order to evaluate the unitarity bound.

From the partial derivative of  $f$  in the region  $y \geq g(x)$ ,

$$\frac{\partial f}{\partial x} = \frac{\partial f_2}{\partial x} / (2 - 2x - y) \tag{C1}$$

one can see that, at fixed  $y$ , the function  $f$  increases monotonously from  $x = 0$  to the point  $x = 1 - y/2$ , where the partial derivative in Eq.(C1) is zero. The points  $x = 1 - y/2$  lie on the straight line  $y_1(x) = 2 - 2x$ . In the range  $1 - y/2 \leq x \leq 1$  the function  $f$  decreases monotonously. Taking into account the symmetry  $f(x;y) = f(y;x)$ , we see that at fixed  $x$  the function  $f$  increases monotonously from  $y = 0$  to the point  $y = 1 - x/2$ , where the partial derivative of  $f$  with respect to  $y$  is zero. These points lie on the straight line  $y_2(x) = 1 - x/2$ . Beyond this line  $f$  decreases monotonously. Note that both straight lines lie in the range of  $f_2$ .

Figure 3 shows a contour plot of the function  $f(x; y)$ , together with the lines  $y_1$  and  $y_2$  which intersect at the point

$$x = y = \frac{2}{3} : \quad (C2)$$

At this point both partial derivatives of  $f$  are equal to zero and therefore the point (C2) corresponds to the absolute maximum of  $f$ , given by

$$f_{\max} = f\left(\frac{2}{3}; \frac{2}{3}\right) = \frac{2}{3^{3-2}} = 0.385 : \quad (C3)$$

This number constitutes the absolute upper bound for  $J_j$ .

## REFERENCES

- [1] C. Athanassopoulos et al., *Phys. Rev. Lett.* 77, 3082 (1996).
- [2] J. Kleinfeller, *Nucl. Phys. B (Proc. Suppl.)* 48, 207 (1996).
- [3] A. Romosan et al., *Phys. Rev. Lett.* 78, 2912 (1997).
- [4] A. De Santo, Talk presented at the XXXI<sup>th</sup> Rencontres de Moriond "Electroweak interactions and Unified Theories", Les Arcs, 15-22 March 1997.
- [5] D. Macina, *Nucl. Phys. B (Proc. Suppl.)* 48, 183 (1996).
- [6] M. Laveder, *Nucl. Phys. B (Proc. Suppl.)* 48, 188 (1996).
- [7] K. S. McFarland et al., *Phys. Rev. Lett.* 75, 3993 (1995).
- [8] R. I. Steinberg, *Proc. of the 5<sup>th</sup> International Workshop on Neutrino Telescopes, Venezia, March 1993.*
- [9] F. Boehm et al., *The Palo Verde experiment, 1996*  
(<http://www.cco.caltech.edu/~songhoon/Palo-Verde/Palo-Verde.html>).
- [10] Y. Suzuki, Talk presented at Neutrino 96, Helsinki, June 1996.
- [11] MINOS Coll., NUM HL-63, February 1995.
- [12] ICARUS Coll., LNGS-94/99-I, May 1994.
- [13] F. Boehm, *Nucl. Phys. B (Proc. Suppl.)* 48, 148 (1996); F. Vannucci, *ibid.*, 154 (1996).
- [14] B. T. Cleveland et al., *Nucl. Phys. B (Proc. Suppl.)* 38, 47 (1995); K. S. Hirata et al., *Phys. Rev. D* 44, 2241 (1991); GALLEX Coll., *Phys. Lett. B* 388, 384 (1996); J. N. Abdurashitov et al., *Phys. Rev. Lett.* 77, 4708 (1996).
- [15] J. N. Bahcall and M. H. Pinsonneault, *Rev. Mod. Phys.* 67, 781 (1995); S. Turck-Chieze et al., *Phys. Rep.* 230, 57 (1993); V. Castellani et al., *Phys. Rep.* 281, 309 (1997); A. Dar and G. Shaviv, *Nucl. Phys. B (Proc. Suppl.)* 48, 335 (1996).
- [16] S. P. Mikheyev and A. Yu. Smirnov, *Yad. Fiz.* 42, 1441 (1985) [*Sov. J. Nucl. Phys.* 42, 913 (1985)]; *Il Nuovo Cimento C* 9, 17 (1986); L. Wolfenstein, *Phys. Rev. D* 17, 2369 (1978); *ibid.* 20, 2634 (1979).
- [17] GALLEX Coll., *Phys. Lett. B* 285, 390 (1992); P. I. Krastev and S. T. Petcov, *ibid.* 299, 99 (1993); N. Hata and P. G. Langacker, *Phys. Rev. D* 50, 632 (1994); G. Fibrentini et al., *ibid.* 49, 6298 (1994).
- [18] V. Barger, R. J. N. Phillips and K. Whisnant, *Phys. Rev. Lett.* 69, 3135 (1992); P. I. Krastev and S. T. Petcov, *Phys. Rev. Lett.* 72, 1960 (1994).
- [19] Y. Fukuda et al., *Phys. Lett. B* 335, 237 (1994); *ibid.* 388, 397 (1996).
- [20] R. Becker-Szendy et al., *Nucl. Phys. B (Proc. Suppl.)* 38, 331 (1995).
- [21] W. W. M. Allison et al., *Phys. Lett. B* 391, 491 (1997).
- [22] B. Achkar et al., *Nucl. Phys. B* 434, 503 (1995).
- [23] L. Borodovsky et al., *Phys. Rev. Lett.* 68, 274 (1992).
- [24] S. M. Bilenky, C. Giunti and W. Grimus, preprint UW ThPh-1996-42 ([hep-ph/9607372](http://hep-ph/9607372)), to appear in *Z. Phys. C*.
- [25] N. Okada and O. Yasuda, preprint TM UP-HEL-9605 ([hep-ph/9606411](http://hep-ph/9606411)).
- [26] M. Taniguchi, *Phys. Rev. D* 55, 322 (1997).
- [27] J. Arifino and J. Sato, *Phys. Rev. D* 55, 1653 (1997); J. Arifino, M. Koike and J. Sato, ICRR-Report-385-97-8 ([hep-ph/9703351](http://hep-ph/9703351)).
- [28] H. Minakata and H. Nunokawa, preprint TM UP-HEL-9704 ([hep-ph/9705208](http://hep-ph/9705208)).
- [29] S. M. Bilenky and B. Pontecorvo, *Phys. Rep.* 41, 225 (1978).

- [30] S.M. Bilenky and S.T. Petcov, *Rev. Mod. Phys.* 59, 671 (1987).
- [31] C.W. Kim and A. Pevsner, *Neutrinos in Physics and Astrophysics, Contemporary Concepts in Physics, Vol. 8*, (Harwood Academic Press, Chur, Switzerland, 1993).
- [32] M. Doi et al., *Phys. Lett. B* 102, 323 (1981); L. Wolfenstein, *Phys. Lett. B* 107, 77 (1981); S.M. Bilenky et al., *Nucl. Phys. B* 247, 61 (1984); B. Kayser, *Phys. Rev. D* 30, 1023 (1984).
- [33] S.M. Bilenky, J. Hosek and S.T. Petcov, *Phys. Lett. B* 94, 495 (1980); M. Doi et al., *Phys. Lett. B* 102, 323 (1981).
- [34] V. Barger et al., *Phys. Rev. D* 22, 1636 (1980); S.M. Bilenky and F. Niedermayer, *Yad. Fiz.* 34, 1091 (1981) [*Sov. J. Nucl. Phys.* 34, 606 (1981)].
- [35] J.T. Peltoniemi and J.W.F. Valle, *Nucl. Phys. B* 406, 409 (1993); D.O. Caldwell and R.N. Mohapatra, *Phys. Rev. D* 50, 3477 (1994); Z. Berezhiani and R.N. Mohapatra, *Phys. Rev. D* 52, 6607 (1995); J.R. Primack et al., *Phys. Rev. Lett.* 74, 2160 (1995); E. Ma and P. Roy, *Phys. Rev. D* 52, R4780 (1995); R. Foot and R.R. Volkas, *Phys. Rev. D* 52, 6595 (1995); E.J. Chun et al., *Phys. Lett. B* 357, 608 (1995); J.J. Gomez-Cadenas and M.C. Gonzalez-Garcia, *Z. Phys. C* 71, 443 (1996); S. Goswami, *Phys. Rev. D* 55, 2931 (1997); A. Yu. Smimov and M. Tanimoto, *Phys. Rev. D* 55, 1665 (1997); E. Ma, *Mod. Phys. Lett. A* 11, 1893 (1996).
- [36] S.M. Bilenky et al., *Phys. Rev. D* 54, 4432 (1996).
- [37] F. Dydak et al., *Phys. Lett. B* 134, 281 (1984).
- [38] I.E. Stockdale et al., *Phys. Rev. Lett.* 52, 1384 (1984).
- [39] S.M. Bilenky et al., *Phys. Lett. B* 356, 273 (1995); *Phys. Rev. D* 54, 1881 (1996).
- [40] L.A. Ahrens et al., *Phys. Rev. D* 36, 702 (1987).
- [41] N. Ushida, *Phys. Rev. Lett.* 57, 2897 (1986).
- [42] C. Jarlskog, in *Proc. of CP Violation*, Ed. C. Jarlskog, *Advanced Series in High Energy Physics Vol. 3* (World Scientific, Singapore, 1989), p. 3.
- [43] S.M. Bilenky, C. Giunti and W. Grimus, in preparation.

## FIGURES

FIG 1. Upper bound for the transition probability of LBL reactor  $\nu_e$ 's into all possible states,  $1 - P_{e\mu}^{(LBL)}$ , for the SBL  $m^2$  in the range  $10^{-1} \text{ eV}^2 < m^2 < 10^3 \text{ eV}^2$ . The solid curve is obtained from the 90% CL exclusion plot of the Bugey  $\nu_e \rightarrow \nu_e$  experiment (see Eq.(4.4)). The dash-dotted and dash-dot-dotted vertical lines depict, respectively, the expected sensitivities of the CHOOZ and Palo Verde LBL reactor neutrino experiments. The shadowed region corresponds to the range of  $m^2$  allowed at 90% CL by the results of the LSND experiment, taking into account the results of all the other SBL experiments (see Eq.(1.4)).

FIG 2. Upper bound for the probability of  $\nu_e \rightarrow \nu_\mu$  and  $\nu_e \rightarrow \nu_\tau$  transitions in LBL experiments. The solid curve is obtained only from the 90% CL exclusion plot of the Bugey  $\nu_e \rightarrow \nu_e$  experiment (see Eq.(4.9)), whereas for the long-dashed curve the 90% CL exclusion plots of the BNL E734, BNL E776 and CCFR  $\nu_e \rightarrow \nu_\mu$  and  $\nu_e \rightarrow \nu_\tau$  experiments (see Eq.(4.6)) and for the short-dashed curve the 90% CL exclusion plots of the CDHS [37] and CCFR [38]  $\nu_e \rightarrow \nu_\mu$  experiments (see Eq.(4.12)) have been used in addition. The dotted, dash-dotted and dash-dot-dotted vertical lines represent, respectively, the expected sensitivities of the LBL accelerator neutrino experiments KEK (SK, MINOS and ICARUS). The darkly shadowed region is allowed by the results of the LSND experiment, taking into account the results of all the other SBL experiments, in the case of LBL oscillations in vacuum. The two horizontal borderlines correspond to the limits (1.4) for  $m^2$  and the left borderline corresponds to the lower bound in Eq.(4.10). The lightly shadowed region is allowed by the results of the LSND and all the other SBL experiments in the case of LBL oscillations in matter. The solid curve constitutes also an upper bound for the probability of  $\nu_e \rightarrow \nu_\mu$  and  $\nu_e \rightarrow \nu_\tau$  transitions.

FIG 3. Contour plot of the function  $f(x;y)$  given in Eq.(5.2). The dotted line is the borderline  $g(x) = 2(1-x) = (2-x)$  between the regions where  $f = f_1$  and  $f = f_2$ . The two solid lines represent the functions  $y_1(x) = 2-2x$  and  $y_2(x) = 1-x=2$ .

FIG 4. Upper bound for the parameter  $jL_e - j$  which characterizes the CP-odd asymmetry in the  $\nu_e \rightarrow \nu_e$  channel for the SBL parameter  $m^2$  in the range  $10^{-1} \text{ eV}^2 < m^2 < 10^3 \text{ eV}^2$ . The solid curve represents the upper function in Eq.(5.4) and is obtained from the 90% CL exclusion plot of the Bugey  $\nu_e \rightarrow \nu_e$  experiment. The dotted curve improves the solid curve where  $a^0 = a_e^0 = 2$  (the lower function in Eq.(5.4)). It is obtained from the 90% CL exclusion plots of the Bugey  $\nu_e \rightarrow \nu_e$  experiment and the CDHS and CCFR  $\nu_e \rightarrow \nu_\mu$  and  $\nu_e \rightarrow \nu_\tau$  experiments. The dash-dotted curve is obtained from the 90% CL exclusion plots of the Bugey  $\nu_e \rightarrow \nu_e$  experiment and the BNL E734, BNL E776 and CCFR  $\nu_e \rightarrow \nu_\mu$  and  $\nu_e \rightarrow \nu_\tau$  experiments (see the upper function in Eq.(5.8)). The shadowed region corresponds to the range (1.4) of  $m^2$  allowed at 90% CL by the results of the LSND experiment. The solid curve represents also an upper bound for  $jL_e - j$ .

FIG 5. Upper bound for the parameter  $j_I - j_J$  which characterizes the CP-odd asymmetry in the  $\mu^+ \mu^-$  channel. The solid curve is obtained from the 90% CL exclusion plots of the CDHS and CCFR  $\mu^+ \mu^-$  and  $\mu^+ \mu^-$  experiments (see Eq.(5.5)). The dotted curve is obtained from the 90% CL exclusion plots of the FNAL E531 and CCFR  $\mu^+ \mu^-$  experiments (see Eq.(5.9)). The shadowed region corresponds to the range (1.4) of  $m^2$  allowed at 90% CL by the results of the LSND experiment.

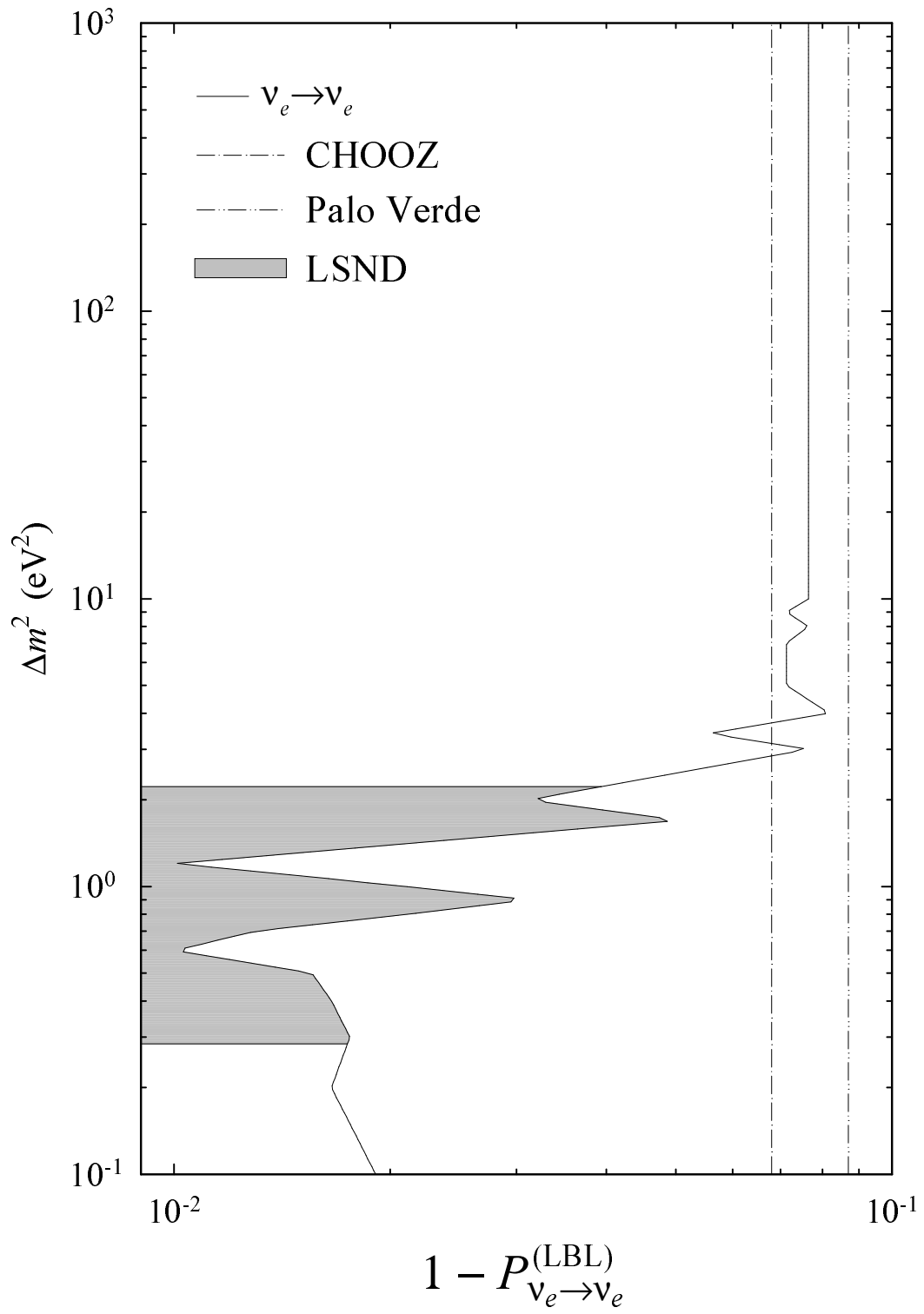


Figure 1

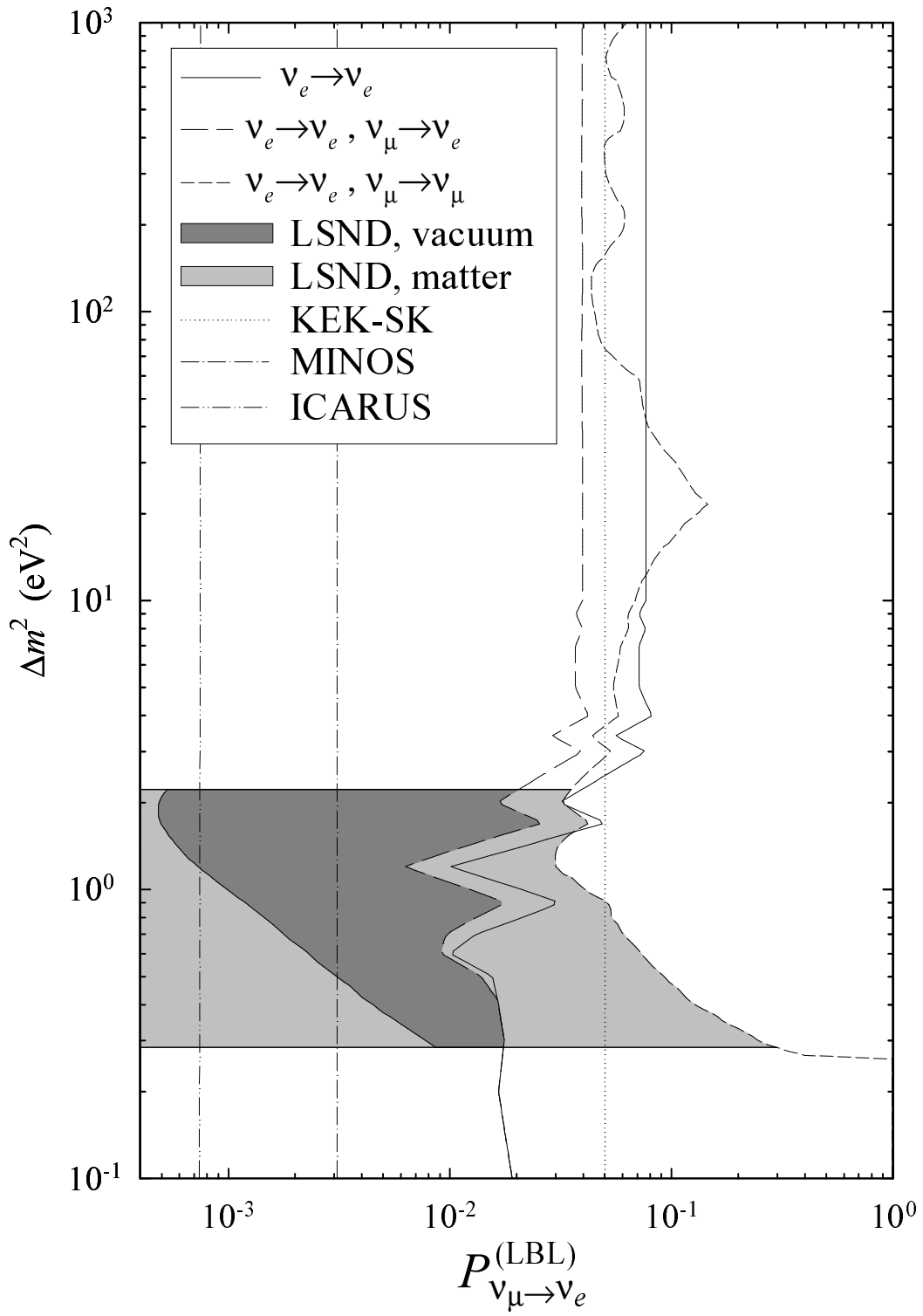


Figure 2

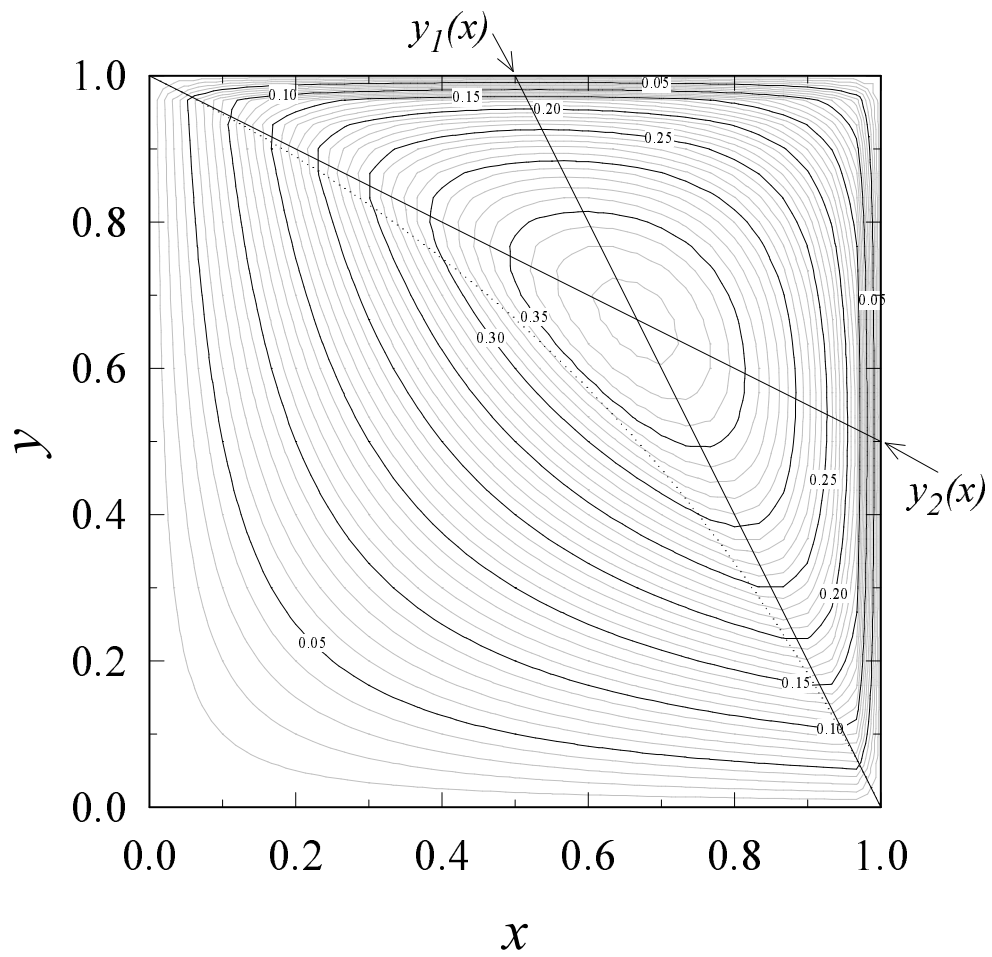


Figure 3

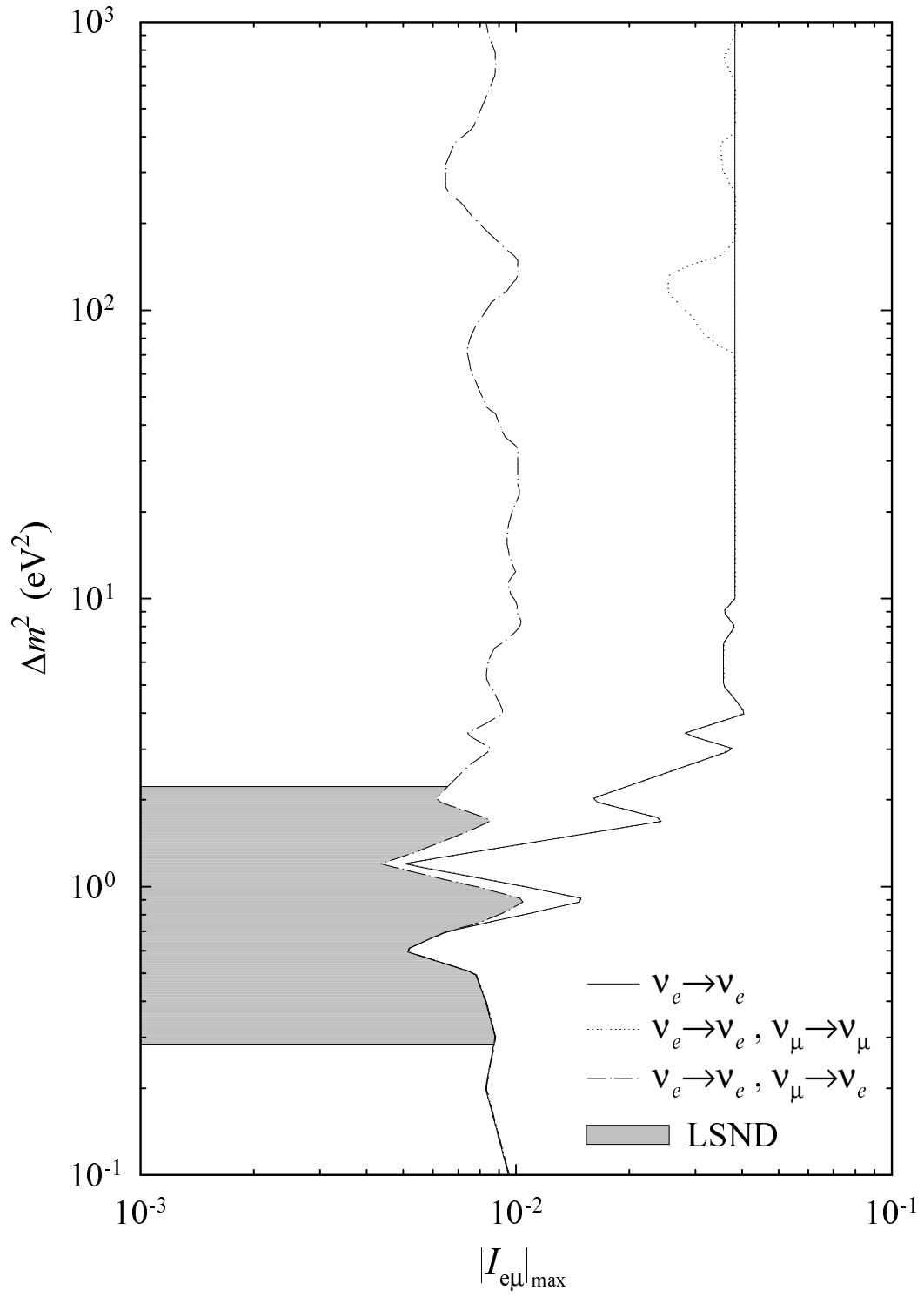


Figure 4

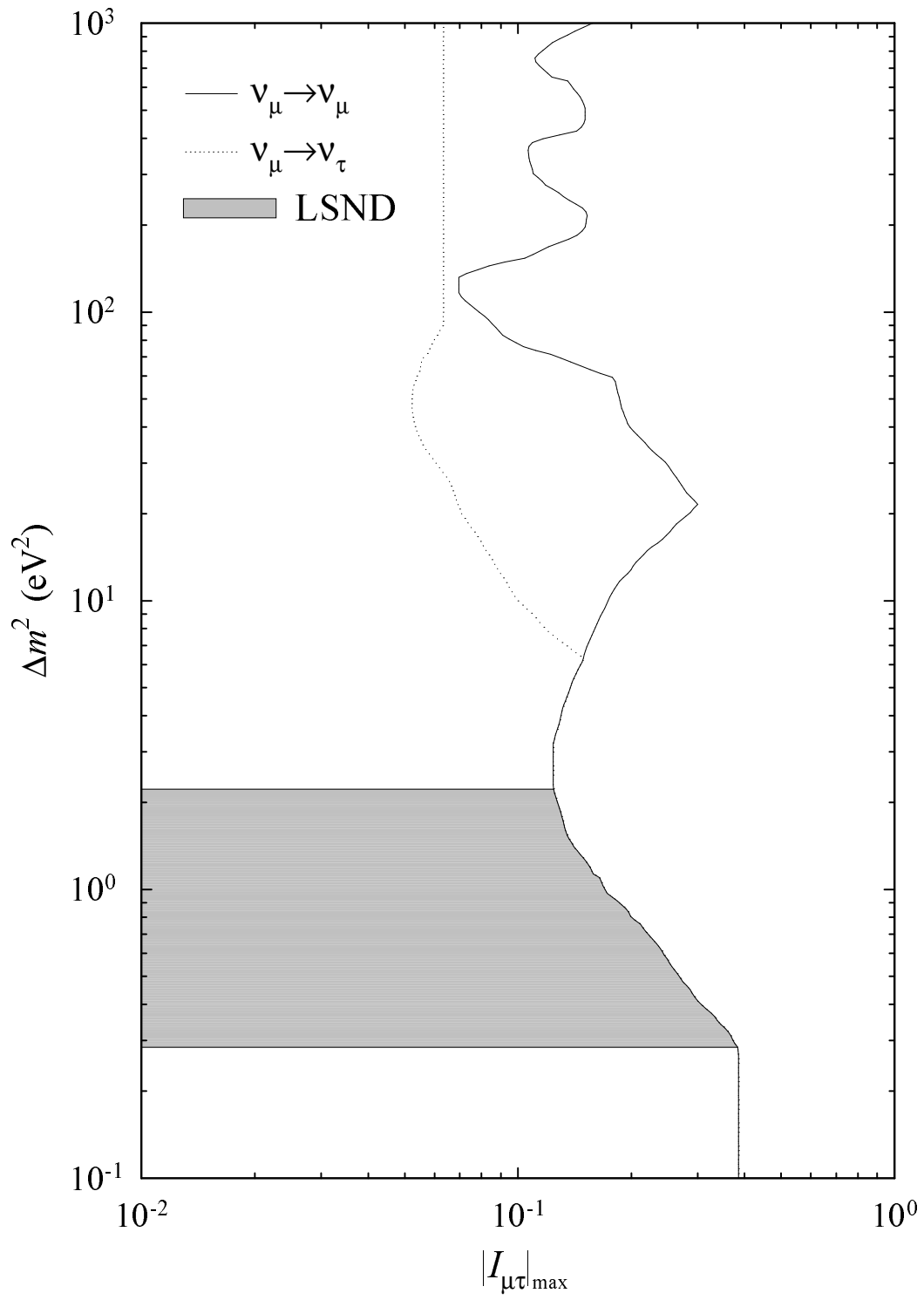


Figure 5